Convergence of IRBIT, phosphatidylinositol (4,5) bisphosphate, and WNK/SPAK kinases in regulation of the Na^+-HCO_3^- cotransporters family

Jeong Hee Hong[a,1], Dongki Yang[b,1], Nikolay Shcheynikov[a], Ehud Ohana[a], Dong Min Shin[c], and Shmuel Muallem[a,2]

[a]Epithelial Signaling and Transport Section, Molecular Physiology and Therapeutics Branch, National Institute of Dental and Craniofacial Research, National Institutes of Health, Bethesda, MD 20892; [b]Department of Physiology, Graduate School of Medicine, Gachon University of Medicine and Science, Incheon 406-799, Korea; and [c]Department of Oral Biology, Brain Korea 21 Project, Yonsei University College of Dentistry, Seoul 120-752, Korea

Edited* by Melanie H. Cobb, University of Texas Southwestern Medical Center, Dallas, TX, and approved January 29, 2013 (received for review December 10, 2012)

Fluid and HCO_3^- secretion is a vital function of secretory epithelia, involving basolateral HCO_3^- entry through the Na^+-HCO_3^- cotransporter (NBC) NBCe1-B, and luminal HCO_3^- exit mediated by cystic fibrosis transmembrane conductance regulator (CFTR) and solute carrier family 26 (SLC26) Cl^-/HCO_3^- exchangers. HCO_3^- secretion is highly regulated, with the WNK/SPAK kinase pathway setting the resting state and the IRBIT/PP1 pathway setting the stimulated state. However, we know little about the relationships between the WNK/SPAK and IRBIT/PP1 sites in the regulation of the transporters. The first 85 N-terminal amino acids of NBCe1-B function as an autoinhibitory domain. Here we have identified a positively charged module within NBCe1-B(37-65) that is conserved in NBCn1-A and all 20 members of the NBC superfamily except NBCe1-A. This module is required for the interaction and activation of NBCe1-B and NBCn1-A by IRBIT and their regulation by phosphatidylinositol 4,5-bisphosphate (PIP_2). Activation of the transporters by IRBIT and PIP_2 is nonadditive but complementary. Phosphorylation of Ser65 mediates regulation of NBCe1-B by SPAK, and phosphorylation of Thr49 is required for regulation by IRBIT and SPAK. Sequence searches using the NBCe1-B regulatory module as a template identified a homologous sequence in the CFTR R domain and Slc26a6 sulfat transporter and antisigma factor antagonist (STAS) domain. Accordingly, the R and STAS domains bind IRBIT, and the R domain is required for activation of CFTR by IRBIT. These findings reveal convergence of regulatory modalities in a conserved domain of the NBC that may be present in other HCO_3^- transporters and thus in the regulation of epithelial fluid and HCO_3^- secretion.

Fluid and HCO_3^- secretion is a vital function of secretory epithelia that involves basolateral HCO_3^- entry through the Na^+-HCO_3^- cotransporter (NBC) NBCe1-B and luminal HCO_3^- exit mediated by the concerted activity of cystic fibrosis transmembrane conductance regulator (CFTR) and members of the solute carrier family 26 (SLC26) transporter family (1). HCO_3^- secretion is osmotically active owing to an influx of Na^+-$2HCO_3^-$ (2, 3) and the exchange of $Cl^-/2HCO_3^-$ by Slc26a6 (4, 5), resulting in net osmolyte secretion in the form of HCO_3^-. HCO_3^- secretion is a highly regulated activity, with several signaling pathways converging to regulate key transporters activity to tune the secretion (1); however, very little is known about the molecular mechanisms that regulate fluid and HCO_3^- secretion, particularly the regulation of NBCe1-B.

NBCe1-B was originally designated pancreatic NBC 1 (6) and was later renamed NBCe1-B as a member of the electrogenic NBCe1 subfamily of the Na^+-coupled bicarbonate transporter (NCBT) superfamily (2, 3). NBCe1-B is is expressed in the basolateral membrane of most secretory epithelia, including the pancreas, salivary glands, airway, and intestines (1). The NCBTs encompass 13 transmembrane domains with varying cytoplasmic N and C termini among the isoforms (3). Most members of the NCBT superfamily have a unique N terminus (the first 85 residues in NBCe1-B) (7). This domain has been shown to function as an autoinhibitory domain (AID) in NBCe1-B (8–10). Very little is known about the regulation of NBCe1-B or other members of the superfamily beyond that NBCe1-B may be modestly activated by cAMP (11, 12), although inhibition of NBCe1-B by cAMP was subsequently reported by the same group (13). NBCe1-B appears to be constitutively phosphorylated by protein kinase A in Thr49 (11); however, its role in activation of the transporter is not clear, given that both the T49A and T49D mutations were found to prevent activation by cAMP (11). Activation of NBCe1-B and NBCe1-C by intracellular Ca^{2+} through an unknown mechanism was reported recently (5). NBCe1-A is activated by phosphatidylinositol 4,5-bisphosphate (PIP_2) (14), but direct activation of NBCe1-B and NBCe1-C by PIP_2 has not been examined. The site of interaction of PIP_2 in regulating the activity of any NCBT family member remains to be determined.

NBCe1-B (9, 10, 15, 16) and NBCe1-C (17) are potently activated by the inositol 1,4,5-triphosphate (IP_3) receptors binding protein released with IP_3 (IRBIT) and are inhibited by the with no lysine kinase (WNK) and Ste20-related proline alanine rich kinase (SPAK) (15). IRBIT also regulates CFTR (15, 16) and sodium-hydrogen exchanger 3 (NHE3) (18). IRBIT activates NBCe1-B by recruiting protein phosphatase 1 (PP1), reversing inhibition by the WNK/SPAK pathway through dephosphorylation of NBCe1-B (15) and relief of inhibition by the AID (9, 10, 15, 16). The WNKs function as scaffolds to recruit SPAK to NBCe1-B, which in turn phosphorylates the transporter at unknown sites. Similarly, the site of IRBIT–AID interaction is unknown. Deletion of the first 16 residues of NBCe1-B prevents activation by IRBIT (9), although the effect of this truncation on IRBIT binding is unclear. On the other hand, an in vitro binding assay revealed binding of IRBIT to NBCe1-B(1-62), but not to NBCe1-B(1-37) (10). This finding suggests that the IRBIT binding site may be located within NBCe1-B(37-62); however, the possible binding of IRBIT to NBCe1-B(37-62) or a site within has not yet been examined.

The extent to which these pathways regulate other members of the NBC family is unknown, although IRBIT may activate an unspecified member of the NBCn1 subfamily (2). The NBCn1 subfamily was established with the discovery of NBC3, later renamed NBCn1-A. NBCn1-A is a widely expressed electroneutral NBC (3, 7) that mediates HCO_3^- salvage in secretory epithelia (19, 20).

Author contributions: J.H.H., D.Y., N.S., D.M.S., and S.M. designed research; J.H.H., D.Y., and N.S. performed research; E.O. contributed new reagents/analytic tools; J.H.H., D.Y., N.S., and S.M. analyzed data; and J.H.H., D.M.S., and S.M. wrote the paper.

The authors declare no conflict of interest.

*This Direct Submission article had a prearranged editor.

[1]J.H.H. and D.Y. contributed equally to this work.

[2]To whom correspondence should be addressed. E-mail: Shmuel.Muallem@nih.gov.

This article contains supporting information online at www.pnas.org/lookup/suppl/doi:10.1073/pnas.1221410110/-/DCSupplemental.

Given that sequence analysis has shown significant conservation of the N termini of NBCe1-B and NBCn1-A, we deemed it useful to compare the regulation of these NBCs by IRBIT/PP1, PIP_2, and SPAK to evaluate the generality of this regulation. In the present studies, we also investigated whether these multiple regulatory pathways converge on the same domain to regulate the transporters.

We have identified a positively charged domain within NBCe1-B (37-65) that is conserved in NBCn1-A and most members of the NCBT superfamily and is required for interaction and activation of the transporters by IRBIT. The same domain mediates regulation of NBCe1-B and NBCn1-A by PIP_2. Importantly, activation of the transporters by IRBIT and PIP_2 is nonadditive but complementary. Phosphorylation of Ser65 within this domain mediates regulation of NBCe1-B by SPAK, and phosphorylation of Thr49 within NBCe1-B(37-65) is required for regulation by the activator IRBIT and the inhibitor SPAK. Moreover, a sequence search using the conserved module identified a similar module in Slc26a6 and CFTR that is required for regulation of CFTR by IRBIT. These findings reveal convergence of regulatory modalities in the AID of the NBCs and thus in the regulation of epithelial fluid and HCO_3^- secretion.

Results and Discussion

Current driven by electrogenic Na^+-HCO_3^- cotransporters has been previously reported only in *Xenopus* oocytes. However, several regulatory functions are absent or are different in the oocytes. Thus, we expressed NBCe1-B in HeLa cells and determined the NBCe1-B–mediated current and changes in intracellular pH (pH_i) to study regulation of NBCe1-B activity in mammalian cells. Exposing HeLa cells transfected with NBCe1-B to solution containing 28 mM HCO_3^- resulted in a small outward current that was absent from cells transfected with GFP (Fig. S1 *A* and *D*). The current was markedly increased by IRBIT (Fig. S1*A*) and inhibited by 0.5 mM diisothiocyanostilbene-2,2′-disulfonic acid (DIDS), an NBCe1-B inhibitor (Fig. S1 *C* and *D*). Similar results were observed when NBCe1-B activity was measured as the influx of Na^+-dependent HCO_3^- into acidified cells (Fig. S1 *E* and *F*).

IRBIT and PIP_2 Sites. The main goal of the present work was to identify the sites for regulation of the NBCs by IRBIT, PIP_2, and the WNK/SPAK pathway and the relationships among these sites. Sites for interaction and regulation by PIP_2 have been reported for several transporters, most of which involve clusters of positively charged residues (21). Sequence analysis of all members of the NCBT superfamily, in which the N termini show significant homology, identified a conserved cluster of positively charged residues (Fig. S2*A*). To examine how this sequence, which is within the AID of NBCe1-B, may interact with IRBIT and PIP_2, we developed a model of the entire NBCe1-B N terminus, consisting of 400 residues (Fig. S2*B*). The N terminus outside the AID is based on the crystal structure of anion exchanger 1 (AE1) (22) and is predicted with high confidence. A similar analysis that reached the same conclusion was reported previously (11). The AID (shown in turquoise in Fig. S2*B*) was predicted with less confidence by ROBETTA using a de novo modeling source. The highly charged cluster (highlighted in orange) is also shown in Fig. 1*A*. Deletion of residues 40–62 in NBCe1-B eliminated NBCe1-B–IRBIT interaction, and NBCe1-B became fully active owing to removal of autoinhibition and was no longer activated by IRBIT (Fig. S3). Thus, we focused on the region around the three arginines highlighted in red in Fig. 1*A* and Fig. S2*B* and eventually on the three arginines themselves, which are conserved in almost all NBC isoforms (Fig. S2*A*).

Single R/A mutations had no effect on the NBCe1-B–IRBIT interaction, whereas the double R42/43A significantly reduced and the the triple R42/43/44A (3R/3A mutant) nearly eliminated this interaction (Fig. 1 *B* and *C*). As expected, the 3R/3A mutant was

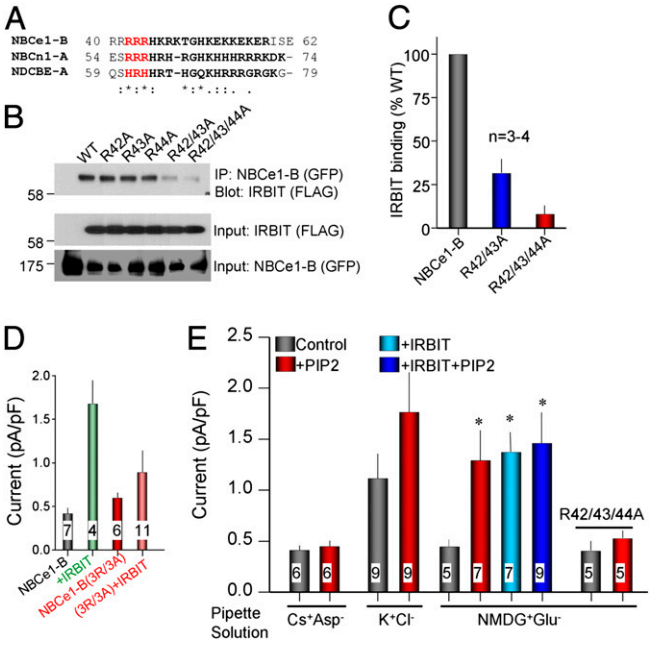

Fig. 1. The NBCe1-B site mediating regulation by IRBIT and PIP_2. (*A*) Alignment of the conserved highly charged N-terminal modules in NBCe1-B, NBCn1-A, and NDCBE-A. The arginines mutated in this study are highlighted in red. (*B* and *C*) Representative blot showing the effects of the single, double, and triple arginine mutations on the NBCe1-B–IRBIT interaction (*B*) and mean ± SEM of four experiments (*C*). Current measured in HeLa cells expressing the NBC of interest. (*D*) Activation of NBCe1-B current by IRBIT and markedly reduced activation of NBCe1-B(3R/3A). (*E*) NBCe1-B current in different pipette solutions. Where indicated, the pipette solution also included 10 μM PIP_2. Note that IRBIT and PIP_2 activated NBCe1-B similarly, and that activation by PIP_2 was eliminated the 3R/3A mutation.

not activated by IRBIT (Fig. 1*D* and Fig. S4 *A* and *B*). NBCe1-B was activated by PIP_2, but this activation was influenced by the intracellular ion composition (Fig. 1*E*). Dialysis with a solution in which the major salt was Cs^+-aspartate$^-$ prevented activation by PIP_2, and the use of a KCl-based solution resulted in variable current. The best results were obtained with an N-methyl-D-glucamine (NMDG)-based solution. Notably, IRBIT and PIP_2 activated NBCe1-B to the same extent, and the activation was nonadditive. Importantly, the 3R/3A mutant was not activated by PIP_2. To assay the regulation of NBCe1-B by PIP_2 under closer to physiological conditions, we examined activation of NBCe1-B–mediated HCO_3^- transport by PIP_2 delivered with the aid of a carrier peptide (*Methods*). We found that the triple mutant was not activated by IRBIT or PIP_2, that PIP_2 activated NBCe1-B, and that the activation by IRBIT and PIP_2 was nonadditive (Fig. S4 *C* and *D*). The assay shown in Fig. S4 can be used to examine regulation of the electroneutral NBCn1-A by PIP_2 (see below).

SPAK Phosphorylation Site. Given that IRBIT antagonizes and reverses the inhibitory effect of SPAK (15), we asked whether NBCe1-B(3R/3A) is still inhibited by SPAK. Surprisingly, although no R/A mutant had an effect on the interaction of NBCe1-B with SPAK (Fig. 2*A*), inhibition of NBCe1-B(3R/3A) by SPAK was lost (Fig. 2 *B* and *C*). We previously showed that SPAK inhibits NBCe1-B by reducing its surface expression. This mechanism is confirmed in Fig. 2*D*, which also shows that surface expression of NBCe1-B(3R/3A) was unaffected by SPAK.

These unexpected findings raise the possibility that SPAK may act by phosphorylating Ser/Thr residues within the AID. Fig. 3*A* shows all of the Ser/Thr residues in NBCe1-B, with those in green having no effect and those in blue (also shown as blue

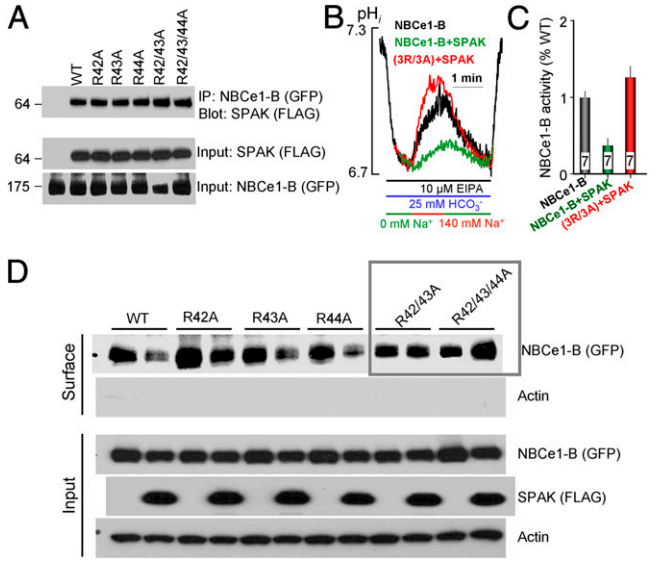

Fig. 2. Effects of the arginine mutations on inhibition of NBCe1-B by SPAK. (*A*) The arginine mutations have no effect on the NBCe1-B–SPAK interaction. (*B* and *C*) NBCe1-B(3R/3A) is not inhibited by SPAK. (*D*) The 3R/3A mutation prevents reduced surface expression of NBCe1-B by SPAK.

sticks in the model in Fig. S2*B*) affecting the activity and/or regulation of NBCe1-B by SPAK. Fig. S5*A* shows the behavior of NBCe1-B(S79A) as an example of a mutant that behaves like WT NBCe1-B. The traces in Fig. 3 *B–D* and the summaries in Fig. 3*E* show the effect of SPAK on NBCe1-B(S65). Ser65 behaved as was expected by a primary serine phosphorylated by SPAK. NBCe1-B(S65A) increased basal activity and was not inhibited by SPAK, suggesting that NBCe1-B is partially inhibited by SPAK under basal conditions, as has been reported for siSPAK in HEK cells and in the pancreatic duct (15). On the other hand, the activity of NBCe1-B(S65D) was lower than that of WT NBCe1-B, reduced to the activity measured with NBCe1-B treated with SPAK, and was not further inhibited by SPAK. The NBCe1-B(S65D) mutation did not prevent activation by IRBIT.

Thr49 is another NBCe1-B–phosphorylatable residue that affected inhibition by SPAK. However, mutations of Thr49 did not result in the behavior expected from a primary SPAK site. Thr49 was previously shown to be constitutively phosphorylated by PKA (11). The NBCe1-B(T49A) and NBCe1-B(T49D) mutants had no effect on basal activity, but similarly prevented inhibition by SPAK and stimulation by IRBIT, rather than demonstrating increased basal activity by NBCe1-B(T49A) and reduced basal activity by NBCe1-B(T49D), while preventing the effects of SPAK (Fig. S5). Thr49 lies within the positively charged cluster, and thus the prevention of the effects of both IRBIT and SPAK by Thr49Ala and Thr49Asp suggests that an intact cluster is required for both activation by IRBIT and inhibition by SPAK. Further support for this idea is provided by the action of the NBCe1-B (T49A/S65A) double mutant, which prevented inhibition by SPAK and activation by IRBIT (Fig. 3*E*).

To further analyze the effect of the Ser/Thr mutations, we examined the effect of the mutations on NBCe1-B phosphorylation and its interaction with SPAK and IRBIT; the results are shown in Fig. 3 *F–H* and Fig. S6. Control experiments showed that the Ser/Thr mutations had no apparent effect on the interaction of NBCe1-B with SPAK (Fig. S6*A*) or IRBIT (Fig. S6*B*). The Ser65Ala mutation prevented reduction of NBCe1-B surface expression by SPAK (Fig. 3*F*), accounting for the lack of NBCe1-B (S65A) activity inhibition by SPAK. The NBCe1-B(S65A) and NBCe1-B(S79A) mutations had no effect on basal phosphorylation, whereas in all experiments the Thr49Ala mutation increased the basal phosphorylation of NBCe1-B to nearly the level observed with SPAK (Fig. 3*G*). The reason for the increased phosphorylation or the residue(s) that are phosphorylated to increase phosphorylation of NBCe1-B(T49A) is not known at present. Accordingly, to best determine the effect of the mutations on NBCe1-B phosphorylation by SPAK, we evaluated the change in phosphorylation caused by SPAK (Fig. 3*H*), which indicated that SPAK did not phosphorylate NBCe1-B(T49A) or NBCe1-B (S65A) but phosphorylated the control NBCe1-B(S79A) similar to NBCe1-B. Taken together, the findings presented in Fig. 3 identify phosphorylation of Ser65 by SPAK as essential to the regulation of the surface expression and thus also the activity of NBCe1-B.

General Role of the Charged Cluster. The presence of a similar motif in the N terminus on NBCe1-B, NBCn1-A, and Na^+-dependent

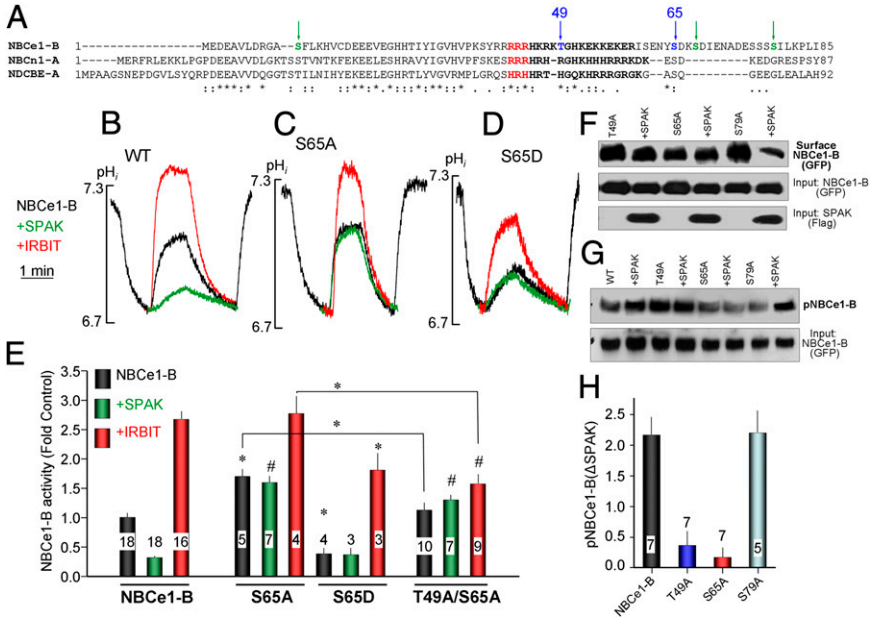

Fig. 3. Identification of the SPAK phosphorylation site in the N terminus of NBCe1-B. (*A*) Alignment of the N terminus 80–90 residues of NBCe1-B, NBCn1-A, and NDCBE-A. The arrows indicate the Ser/Thr residues mutated in this study. They were selected based on conservation among the transporters (Ser12) known to be phosphorylated (Thr49), to be close to Ser65 (Ser68), or to be part of a cluster (S79). The green arrows mark the Ser residues that were mutated and had no effect on activity. Mutation of the residues in blue altered the effect of IRBIT and/or SPAK. (*B–E*) Example traces for WT (*B*) and the indicated mutants (*C* and *D*) and the summary of the indicated number of experiments (*E*) for the NBCe1-B mutants alone (black column), and coexpressed with SPAK (green columns) or IRBIT (red columns). *$P < 0.05$ or better relative to the respective WT NBCe1-B. #$P < 0.05$ or better with IRBIT and SPAK. In the case of NBCe1-B(T49A/S65A), the *P* level is relative to the indicated single mutants. (*F–H*) The effect of Ser/Thr mutation on phosphorylation of NBCe1-B by SPAK. The S65A mutation prevented the reduction of NBCe1-B surface expression by SPAK (*F*), and the T49A and S65A mutations markedly reduced phosphorylation of NBCe1-B by SPAK.

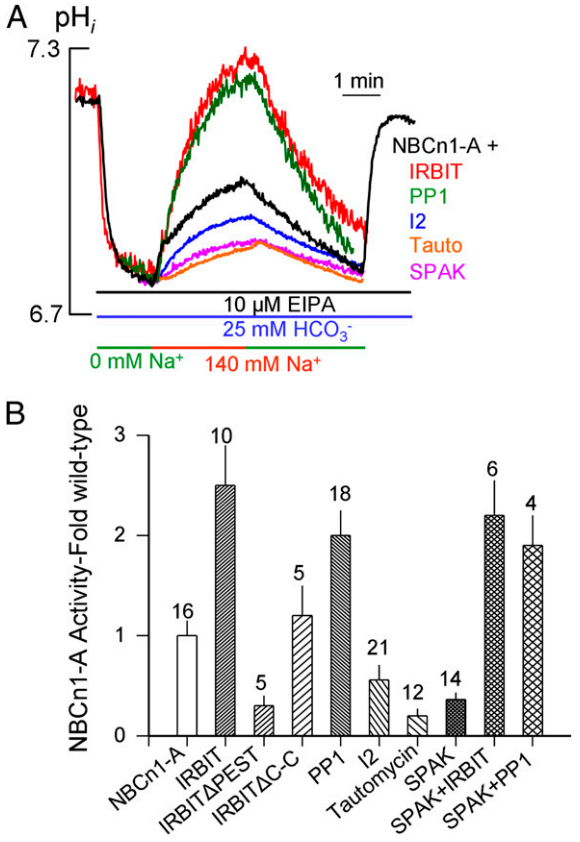

Fig. 4. Regulation of NBCn1-A by the WNK/SPAK and IRBIT/PP1 pathways. (*A*) Sample traces. (*B*) Summary of data, showing that NBCn1-A is activated by IRBIT and PP1, but not by IRBIT(ΔPEST) or IRBIT(ΔC-C), and is inhibited by the PP1 inhibitors I2 and tautomycin. NBCn1-A is inhibited by SPAK, and this inhibition is reversed by IRBIT and PP1.

Cl^-/HCO_3^- exchanger (NDCBE-A) allowed us to examine the generality of regulation by the IRBIT/PP1, PIP_2, and WNK/SPAK pathways. To do so, we first established the activation of NBCn1-A by IRBIT and PP1, inhibition by dominant-negative IRBIT (IRBITΔPEST and IRBITΔC-C) and inhibitors of PP1 (I2 and tautomycin), and inhibition by SPAK and its reversal by IRBIT and PP1 (Fig. 4). These regulatory features are similar to those for NBCe1-B (15). We then analyzed the effects of mutating the three conserved arginines on regulation by IRBIT, PIP_2, and SPAK. We found that NBCn1-A was activated by PIP_2, and that activation by PIP_2 was nonadditive with activation by IRBIT (Fig. 5 *A* and *C*). Significantly, mutation of the conserved 56RRR58 to Ala eliminated activation by IRBIT and PIP_2 (Fig. 5 *B* and *C*) and markedly reduced the NBCn1-A–IRBIT interaction (Fig. 5*D*). Finally, SPAK reduced the surface expression of NBCn1-A (Fig. 5*E*), accounting for the inhibition of NBCn1-A activity by SPAK (Fig. 4). The effect of SPAK on surface expression was reversed by IRBIT and prevented by the 3R/3A mutation (Fig. 5*E*). The WNK/SPAK and IRBIT/PP1 pathways likely regulate the function of NDCBE as well. These findings suggest a general regulatory mechanism of the Na^+-HCO_3^- cotransport with AID that is mediated by the conserved charged motif.

Considering that the WNK/SPAK and IRBIT/PP1 pathways regulate CFTR activity (15, 16), we asked whether the module identified in the NBCs AID is present in CFTR and other transporters. A sequence search using the module as a template identified the sequences shown in Fig. 6*A* in the CFTR R domain and Slc26a6 sulfat transporter and antisigma factor antagonist (STAS) domain. Initial analysis showed that deletion of the R domain almost eliminated CFTR–IRBIT interaction (Fig. 6*B*), the R domain strongly bound IRBIT (Fig. 6*C*), and the STAS domain strongly bound IRBIT (Fig. 6*D*). We could not test the functional consequence of binding of IRBIT to the STAS domain, because deletion within the Slc26a6 STAS domain tested trapped the protein in the endoplasmic reticulum.

Although deletion of the R domain reduces its surface expression, some ΔR-CFTR travels to the plasma membrane, where it behaves as a constitutively active, cAMP-independent Cl^- channel (21, 23). This behavior allowed us to test the role of the R domain in the activation of CFTR by IRBIT. We found that IRBIT activated the current of full-length CFTR that was inhibited by the specific CFTR inhibitor $CFTR_{inh\text{-}172}$ (Fig. 6 *E* and *F*), confirming previously reported results (16). Importantly, the largely constitutive current of ΔR-CFTR was inhibited by 5 μM $CFTR_{inh\text{-}172}$, and the activity of ΔR-CFTR was not activated by IRBIT (Fig. 6 *E* and *F*). These interesting findings suggest that the regulatory module identified in the present work may be a general module that integrates regulatory modalities in other transporters involved in fluid and electrolyte secretion in secretory epithelia.

Conclusions

The present findings identify a regulatory module within the N terminus of the majority of the NBCs in the NCBT superfamily (16 of 25 isoforms) that may be present in other transporters as well. Importantly, key regulatory modalities are congregated within the module to regulate both the inhibition and activation of electrogenic and electroneutral NBCs. Indeed, this module has been shown to function as an autoinhibitory domain (2) that keeps the transporters, and thus the secretion/salvage mediated by these transporters, in an inactive state. Our findings suggest that recruitment of SPAK by the WNK kinases to these transporters stabilizes autoinhibition by the AID, given that mutations of Ser65 that are phosphorylated by SPAK affect basal activity, increasing activity by Ser/Ala mutations and suppressing activity by Ser/Asp mutations. This autoinhibitory state was reversed by

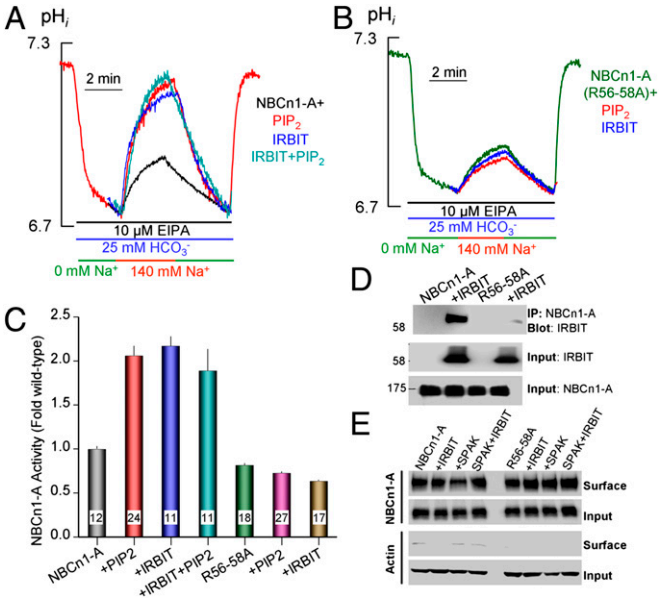

Fig. 5. Effects of the arginine mutations on activation of NBCn1-A by IRBIT and PIP_2. (*A–C*) Activation of NBCn1-A by IRBIT and PIP_2 is nonadditive (*A* and *C*) and is eliminated by the 3R/3A mutation (*B* and *C*). (*D*) The NBCn1-A (3R/3A) mutation also prevents interaction with IRBIT. (*E*) SPAK reduces surface expression of NBCn1-A, which is reversed by IRBIT, and the effect of SPAK on surface expression is eliminated by the 3R/3A mutation.

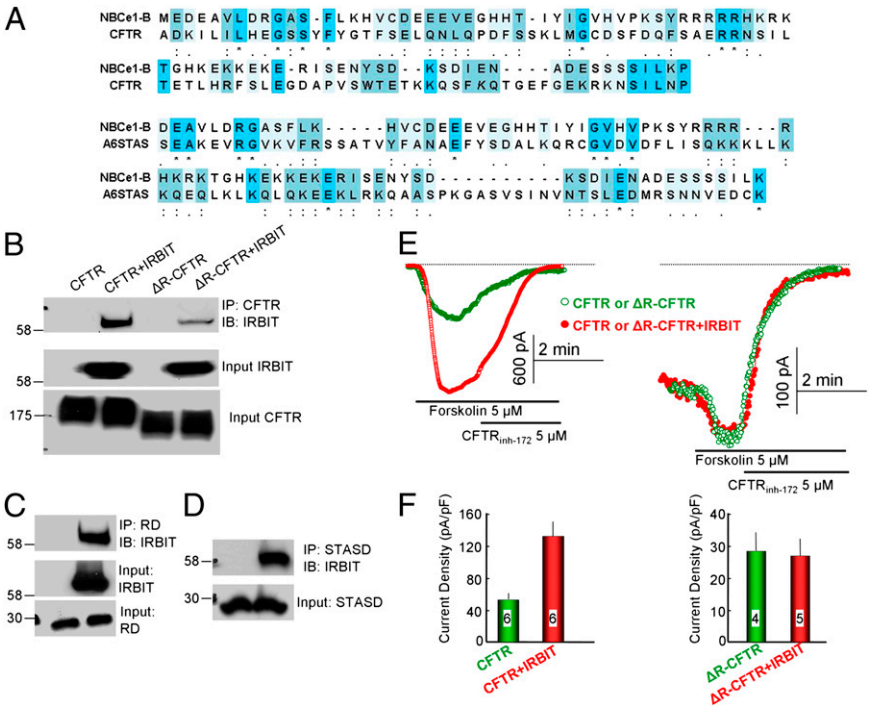

Fig. 6. CFTR and Slc26a6 sites that mediate regulation by IRBIT. (*A*) The sequence within the CFTR R domain and the sequence within the Slc26a6 STAS domain that show significant homology with the NBC regulatory module, identified using the sequence in Fig. 1*A* as a template. (*B*) Deletion of the R domain inhibits CFTR–IRBIT interaction. (*C*) The R domain (RD) interacts with IRBIT. (*D*) IRBIT interacts with the Slc26a6 STAS domain. (*E*) Current traces in HEK cells expressing CFTR (*Left*) or ΔR-CFTR (*Right*) and with and without IRBIT and stimulated with 5 μM forskolin. The CFTR current is potently activated by IRBIT. The ΔR-CFTR current is minimally activated further by forskolin and is inhibited by CFTR$_{inh-172}$, but is not activated by IRBIT. (*F*) Mean ± SEM of experimental data.

both IRBIT and PIP_2. We were somewhat surprised to find that the functions of IRBIT and PIP_2 are nonadditive but appear to be complementary, owing to their interaction with the same positively charged conserved arginines within the AID. IRBIT and IP_3 are known to compete for binding to the IP_3-binding pocket of the IP_3 receptors (24), and we found that IRBIT and the IP_3 containing PIP_2 interacted with the same site in the AID of the NBCs. The complementary action of PIP_2 may serve as a backup mechanism to ensure activation of the transporters on demand; however, it is more likely that under physiological conditions, both mechanisms cooperate to regulate the activity of the transporters, thereby increasing the fidelity of the activated state. The identification of a similar module in CFTR and Slc26a6 raises the possibility that this module may function in other transporters as well. Exploring the roles of this module in the various transporters and in the regulation of epithelial transport will be of interest.

Methods

Plasmid Construction and Solutions. The p3xFLAG-CMV-7.1/IRBIT, pEGFP-C1/NBCe1-B, pCDNA 3.1+/NBCn1-A, and ΔR-CFTR constructs have been described previously (16, 23, 25). The arginine mutants and deletions in NBCe1-B and NBCn1-A were generated by PCR with Pfu DNA polymerase (Agilent), using primers to change specific regions. All constructs were verified by determining the insert size after treatment with restriction enzyme and sequencing of the entire ORFs to ensure the absence of unwanted mutations. The standard bath solution (solution A) contained 140 mM NaCl, 5 mM KCl, 1 mM $MgCl_2$, 1 mM $CaCl_2$, 10 mM Hepes (pH 7.4 with NaOH), and 10 mM glucose. Na^+-free solutions were prepared by replacing Na^+ with NMDG. HCO_3^--buffered solutions were prepared by replacing 25 mM Na^+ anion with 25 mM Na^+-HCO_3^- and reducing Hepes to 2.5 mM. HCO_3^--buffered solutions were gassed with 5% (vol/vol) CO_2 and 95% (vol/vol) O_2. The osmolarity of all solutions was adjusted to 310 mOsmol with the major salt.

pH_i Measurements. pH_i was measured with 2′,7′-bis-(carboxyethyl)-5-(and-6)-carboxyfluorescein (BCECF) (Teflab) by recording BCECF fluorescence at dual-excitation wavelengths of 490 and 440 nm and collecting the light emitted at wavelengths above 530 nm. HeLa cells grown on coverslips and transfected with the indicated plasmids were loaded in the chamber with BCECF through a 10-min incubation at room temperature with 5 μM BCECF/AM. Subsequent pH measurements were at 37 °C. After stabilization of the fluorescence, the cells were perfused with solution A for at least 10 min before start of pH_i measurements. NBC activity was measured by incubating the cells with 10 μM S-(*N*-ethyl-*N*-isopropyl) amiloride to inhibit all Na^+/H^+ exchangers and in Na^+-free, HCO_3^--buffered media to acidify the cytosol. NBC activity was initiated by perfusing the cells with HCO_3^--buffered media containing 140 mM Na^+. NBC activity was determined from the slopes of first derivatives of the first 30–45 s of pH_i increase and is expressed as percent fold change relative to the activity measured with WT NBCs in the same experiments.

Intracellular Delivery of PIP_2 in Intact Cells. To deliver PIP_2, a mixture of histone H1 carriers and PIP_2 di-C_{16} (obtained from Echelon) at a 1:1 molar ratio was briefly vortexed and then incubated for 10 min at room temperature, according to the manufacturer's instructions. Once formed, the complex was diluted to the desired final concentration of 10 μM with cell culture media. The cells were incubated with the mixture for 50 min at 37 °C in a humidified incubator before loading with BCECF and measurement of pH_{in}.

Surface Expression and Coimmunoprecipitation. For biotinylation experiments to determine transporter surface expression, cells were incubated with 0.5 mg/mL EZ-LINK Sulfo-NHS-LC-biotin (Thermo Scientific) for 30 min at 0 °C, incubated with 100 mM glycine for 10 min, washed with PBS, and lysed. Biotinylated NBCe1-B and NBCn1-A were isolated with avidin beads via incubation of lysates for 2 h at room temperature and then recovered by heating at 37 °C for 30 min. Lysates were prepared by disruption of cells in ice-cold lysis buffer for 15–30 min and collection by centrifugation for 20 min. The lysis buffer contained 20 mM Tris, 150 mM NaCl, 2 mM EDTA, 1% (vol/vol) Triton X-100, and a protease inhibitor mixture. For analysis of phosphoproteins, the lysis buffer was supplemented with a phosphatase inhibitor mixture.

For coimmunoprecipitation, extracts were incubated with anti-Flag and anti–β-actin (Sigma-Aldrich), anti-GFP (Invitrogen), and anti–NBCn1-A (Abcam) antibodies and incubated with protein G Sepharose beads (Invitrogen) for 2 h at 0 °C. Beads were collected and washed three times with lysis buffer, and proteins were recovered by heating in SDS sample buffer at

PHYSIOLOGY

37 °C for 30 min. The heated samples were subjected to SDS/PAGE and subsequently transferred to nitrocellulose membranes.

NBCe1-B Current Measurement in HeLa Cells. NBCe1-B activity was measured in transiently transfected HeLa cells by whole-cell current recording at room temperature. In brief, HeLa cells transfected with NBCe-1 B and with or without IRBIT were plated on 35-mm Petri dishes on the day of the experiment and incubated with culture media for at least 2 h to allow attachment to the dish. Patch clamp pipettes were pulled from glass capillaries (G120F-3; Warner Instruments) using a vertical puller (model PC-10; Narishige). These pipettes had a resistance of 5–7 mega-Ω when filled with KCl-based pipette solution. A reference Ag-AgCl electrode was connected to the bath solution via an agar bridge filled with 140 mM KCl. The current was obtained by rapid (400 ms) alternation of membrane potential from −60 to +60 mV every 2 s from a holding potential of 0 mV. The current recorded at −60 mV was used to calculate current density as pA/pF. An Axopatch 200B patch-clamp amplifier and Digidata 1440A and pClamp 10 software (all from Molecular Devices) were used for data acquisition and analysis. The whole-cell currents were filtered at 1 kHz and sampled at 10 kHz. The cell capacitance was 15–25 pF. The pipette solutions contained 140 mM CsCl, 2 mM MgCl, 1 mM ATP, 0.2 mM EGTA and 10 mM Hepes (adjusted to pH 7.3 with CsOH), or with the major salts replaced with 140 mM KCl, 0.2 mM EGTA, and 10 mM Hepes (adjusted to pH 7.3 with KOH) or 140 mM NMDG-Glu, 10 mM NMDG-Cl, 0.2 mM EGTA, and 10 mM Hepes. The Hepes-buffered bath solution contained 140 mM NaCl, 5 mM KCl, 1 mM $MgCl_2$, 1 mM $CaCl_2$, 10 mM glucose, and 10 mM Hepes (adjusted to pH 7.4 with NaOH). The HCO_3^--buffered solution was prepared by replacing 25 mM NaCl with an equimolar amount of $NaHCO_3$, and the solution was equilibrated with 5% (vol/vol) CO_2/95% (vol/vol) O_2. All experiments were performed at room temperature.

Measurement of ΔR-CFTR Current. The CFTR and ΔR-CFTR current was measured in HEK cells transfected with the indicated plasmid exactly as described previously (16, 23). Stock solution of water-soluble PIP_2 (1 mM) was prepared in deionized water and stored at −20 °C under argon until use. The PIP_2 derivative P-4506 was obtained from Ethelon Biosciences. Fresh PIP_2 was added to the pipette solution, and NBCe1-B activity was measured 2 min after the whole-cell configuration was established. A 100 mM stock solution of DIDS (Molecular Probes) dissolved in DMSO was freshly prepared and diluted to a final concentration of 50 μM in the relevant solutions.

Statistics. All results are given as mean ± SEM. Significance was analyzed using the Student *t* test or ANOVA.

Structural Prediction and Protein Modeling. The entire N terminus of human NBCe1-B, consisting of 400 amino acids (National Center for Biotechnology Information reference sequence NP_001091954), was submitted to the ROBETTA online full-chain protein structure prediction server (26). According to the server parsing hierarchy protocol, the "Ginzu" domain prediction method was used initially, and assigned two domains separated by a cut-linker around residues 81–82. One domain spanning residues 82–400 was identified by "blast" to be homologous to the cytoplasmic domain of the human erythrocyte band 3 cytoplasmic domain (Protein Data Bank ID code 1HYN), with a confidence score of 57.00. No homology was identified for residues 1–81, and thus these were assigned as a multiple sequence alignment cluster by the server for de novo modeling. A de novo model for residues 1–81 was generated (confidence score, 2.095). Five final models were generated by an assembly of the two domains and side chain repacking. The models were very similar, with differences in the tilt of the AID. We selected the model in which the AID was linked to the homologous domain with a hinge that might allow rotation during activation by IRBIT. The coordinates provided by the ROBETTA server were used to generate the final model (Fig. S2*B*) with PyMol software (Schrödinger).

ACKNOWLEDGMENTS. This work was funded by the National Institutes of Health, National Institute of Dental and Cranial Research Intramural Research Program (Grant Z1A-DE000735); the National Research Foundation of Korea (Grant NRF-2009-352-E00046, funded by the Korean Government); and the National Research Foundation of Korea's Basic Science Research Program funded by the Ministry of Education, Science and Technology (Grants 2012-0003965 and 2012R1A2A1A01003487).

1. Lee MG, Ohana E, Park HW, Yang D, Muallem S (2012) Molecular mechanism of pancreatic and salivary gland fluid and HCO_3 secretion. *Physiol Rev* 92(1):39–74.
2. Boron WF, Chen L, Parker MD (2009) Modular structure of sodium-coupled bicarbonate transporters. *J Exp Biol* 212(Pt 11):1697–1706.
3. Pushkin A, Kurtz I (2006) SLC4 base (HCO_3^-, CO_3^{2-}) transporters: Classification, function, structure, genetic diseases, and knockout models. *Am J Physiol Renal Physiol* 290(3):F580–F599.
4. Ohana E, Yang D, Shcheynikov N, Muallem S (2009) Diverse transport modes by the solute carrier 26 family of anion transporters. *J Physiol* 587(Pt 10):2179–2185.
5. Chivian D, Baker D (2006) Homology modeling using parametric alignment ensemble generation with consensus and energy-based model selection. *Nucleic Acids Res* 34(17):e112.
6. Abuladze N, et al. (1998) Molecular cloning, chromosomal localization, tissue distribution, and functional expression of the human pancreatic sodium bicarbonate cotransporter. *J Biol Chem* 273(28):17689–17695.
7. Choi I, Romero MF, Khandoudi N, Bril A, Boron WF (1999) Cloning and characterization of a human electrogenic Na^+-HCO_3^- cotransporter isoform (hhNBC). *Am J Physiol* 276(3 Pt 1):C576–C584.
8. McAlear SD, Liu X, Williams JB, McNicholas-Bevensee CM, Bevensee MO (2006) Electrogenic Na/HCO_3 cotransporter (NBCe1) variants expressed in *Xenopus* oocytes: Functional comparison and roles of the amino and carboxy termini. *J Gen Physiol* 127 (6):639–658.
9. Lee SK, Boron WF, Parker MD (2012) Relief of autoinhibition of the electrogenic Na-HCO(3) [corrected] cotransporter NBCe1-B: Role of IRBIT vs. amino-terminal truncation. *Am J Physiol Cell Physiol* 302(3):C518–C526.
10. Shirakabe K, et al. (2006) IRBIT, an inositol 1,4,5-trisphosphate receptor-binding protein, specifically binds to and activates pancreas-type Na^+/HCO_3^- cotransporter 1 (pNBC1). *Proc Natl Acad Sci USA* 103(25):9542–9547.
11. Chivian D, et al. (2005) Prediction of CASP6 structures using automated Robetta protocols. *Proteins* 61(Suppl 7):157–166.
12. Bachmann O, et al. (2003) cAMP-mediated regulation of murine intestinal/pancreatic Na^+/HCO_3^- cotransporter subtype pNBC1. *Am J Physiol Gastrointest Liver Physiol* 284(1):G37–G45.
13. Chivian D, et al. (2003) Automated prediction of CASP-5 structures using the Robetta server. *Proteins* 53(Suppl 6):524–533.
14. Wu J, McNicholas CM, Bevensee MO (2009) Phosphatidylinositol 4,5-bisphosphate (PIP2) stimulates the electrogenic Na/HCO_3 cotransporter NBCe1-A expressed in *Xenopus* oocytes. *Proc Natl Acad Sci USA* 106(33):14150–14155.
15. Yang D, et al. (2011) IRBIT governs epithelial secretion in mice by antagonizing the WNK/SPAK kinase pathway. *J Clin Invest* 121(3):956–965.
16. Yang D, et al. (2009) IRBIT coordinates epithelial fluid and HCO_3^- secretion by stimulating the transporters pNBC1 and CFTR in the murine pancreatic duct. *J Clin Invest* 119(1):193–202.
17. Yang D, Shcheynikov N, Muallem S (2011) IRBIT: It is everywhere. *Neurochem Res* 36 (7):1166–1174.
18. He P, Zhang H, Yun CC (2008) IRBIT, inositol 1,4,5-triphosphate (IP3) receptor-binding protein released with IP3, binds Na^+/H^+ exchanger NHE3 and activates NHE3 activity in response to calcium. *J Biol Chem* 283(48):33544–33553.
19. Lee MG, et al. (2000) Na(+)-dependent transporters mediate HCO(3)(−) salvage across the luminal membrane of the main pancreatic duct. *J Clin Invest* 105(11):1651–1658.
20. Luo X, et al. (2001) HCO_3^- salvage mechanisms in the submandibular gland acinar and duct cells. *J Biol Chem* 276(13):9808–9816.
21. Ostedgaard LS, Baldursson O, Welsh MJ (2001) Regulation of the cystic fibrosis transmembrane conductance regulator Cl^- channel by its R domain. *J Biol Chem* 276(11):7689–7692.
22. Berridge MJ, Bootman MD, Roderick HL (2003) Calcium signalling: Dynamics, homeostasis and remodelling. *Nat Rev Mol Cell Biol* 4(7):517–529.
23. Ko SB, et al. (2004) Gating of CFTR by the STAS domain of SLC26 transporters. *Nat Cell Biol* 6(4):343–350.
24. Ando H, et al. (2006) IRBIT suppresses IP3 receptor activity by competing with IP3 for the common binding site on the IP3 receptor. *Mol Cell* 22(6):795–806.
25. Park M, et al. (2002) The cystic fibrosis transmembrane conductance regulator interacts with and regulates the activity of the HCO_3^- salvage transporter human Na^+-HCO_3^- cotransport isoform 3. *J Biol Chem* 277(52):50503–50509.
26. Kim DE, Chivian D, Baker D (2004) Protein structure prediction and analysis using the Robetta server. *Nucleic Acids Res* 32(Web Server issue):W526–W531.